Pictorial Essay

Ocular Sonography

M. M. J. McNicholas,[1,2] D. P. Brophy,[1] W. J. Power,[3,4] and J. F. Griffin[1,3]

High-frequency ocular sonography is the ideal method for imaging the eye and intraocular structures. In the presence of opaque ocular media, a complete view of the fundus may be impossible ophthalmoscopically, and in these cases sonography is invaluable. Although high field strength MR imaging with surface coils provides excellent detail of normal and pathologic ocular structures, major shortcomings are lack of spatial resolution and poor specificity with certain lesions. Sonography is superior to CT or MR imaging in detecting ocular lesions such as small melanomas that are 2 mm or less in thickness [1]. The eye can be examined dynamically during eye movements, which is of value in localizing abnormalities [2]. The sonographic appearance of a variety of ocular pathologic conditions is illustrated in this essay.

Technique

The eye is examined through the closed eyelid with a high-frequency probe (usually 10 MHz). The posterior aspect of the globe is assessed with the gain settings adjusted to dampen near field echoes and enhance far field echoes. The near field gain is turned up to assess the vitreous and central part of the globe (Figs. 1 and 2). The globe is examined in the neutral position and during gentle eye movements from left to right.

Normal Anatomy

Although the normal lens reflects the ultrasound beam from the midportions of its anterior and posterior surfaces, its center is anechoic (Fig. 1B). The iris is seen as an echogenic line on either side. The vitreous is anechoic, and the retina is the posterior echogenic limit of the globe. Behind the globe, the retrobulbar fat is echogenic. The optic nerve is seen as a hypoechoic structure extending away from the globe posteriorly. A certain number of echoes may be seen in the vitreous; these are vitreous opacities and are seen with increased frequency with advancing age.

Lens

A cataract may produce echoes in the normally anechoic lens, or the entire margin of the lens may be thickened (Fig. 3). The lens may rupture or become dislocated as a result of trauma (Fig. 4).

Vitreous

Posterior detachment of the vitreous is an age-related phenomenon where the posterior vitreous capsule detaches from the underlying retina (Fig. 5). Occasionally, when detachment

Received February 3, 1994; accepted after revision April 15, 1994.
Presented in part at combined meeting of the Royal College of Radiologists, London, and Faculty of Radiologists, Royal College of Surgeons in Ireland, Dublin, Ireland, September 1991.
[1]Department of Radiology, University College Dublin and St. Vincent's Hospital, Elm Park, Dublin 4, Ireland. Address correspondence to J. F. Griffin.
[2]Present address: Department of Radiology, Massachusetts General Hospital, 32 Fruit St., Boston, MA 02114.
[3]Department of Ophthalmology, Royal Victoria Hospital, Adelaide Rd., Dublin 2, Ireland.
[4]Present address: Massachusetts Eye and Ear Infirmary, Charles St., Boston, MA 02114.

AJR **1994;163:921–926** 0361–830X/94/1634–921

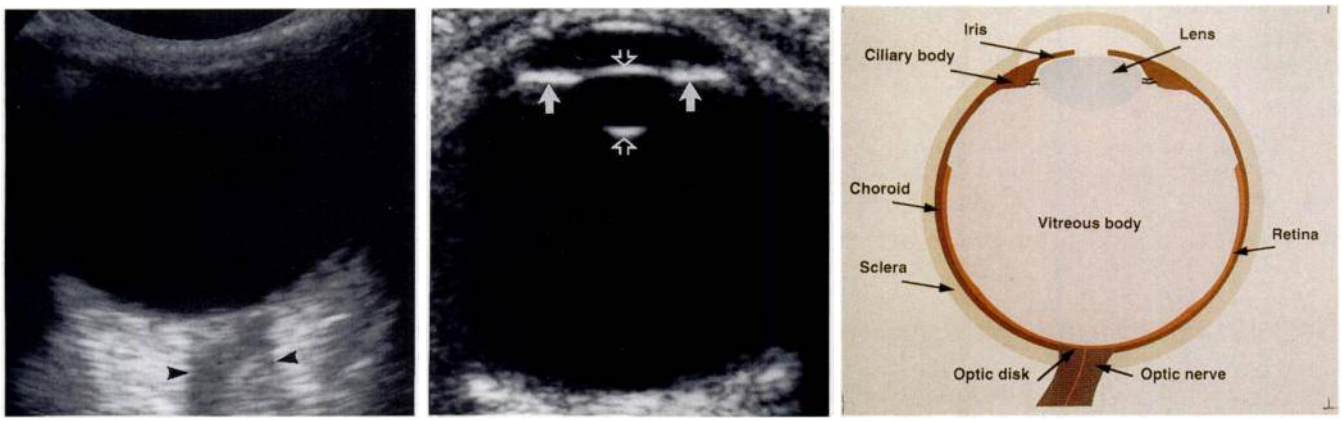

Fig. 1.—Normal eye.
***A*, Axial sonogram after gain settings were adjusted to assess retina and posterior structures. Retina is flat, vitreous is anechoic, and optic nerve *(arrowheads)* is hypoechoic structure extending posteriorly from globe.**
***B*, Axial sonogram shows anterior and posterior surfaces of lens (*open arrows*). Iris is seen on either side (*solid arrows*).**
***C*, Schematic axial cross-section of eye showing some anatomic features that can be seen with sonography.**

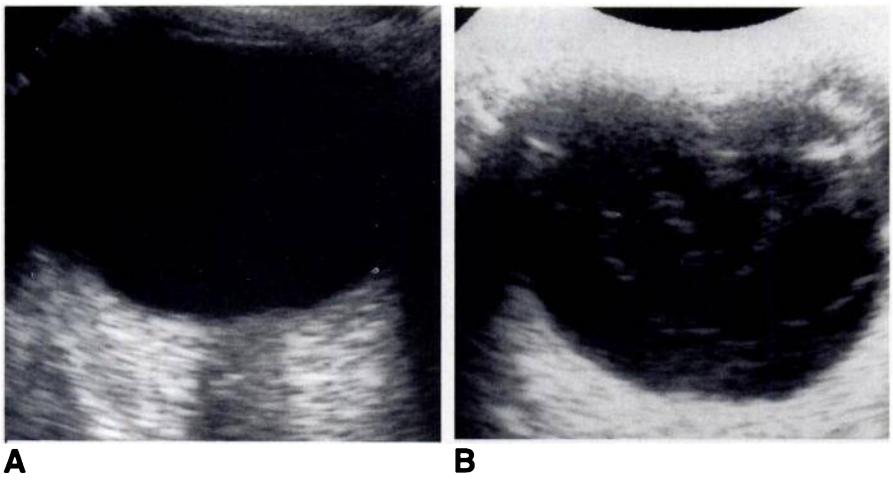

Fig. 2.—Gain settings.
***A*, Axial sonogram with gain settings selected to assess posterior structures. Vitreous is clear.**
***B*, Axial sonogram of same patient, after near field gain was increased to assess vitreous, shows vitreous exudate and stranding.**

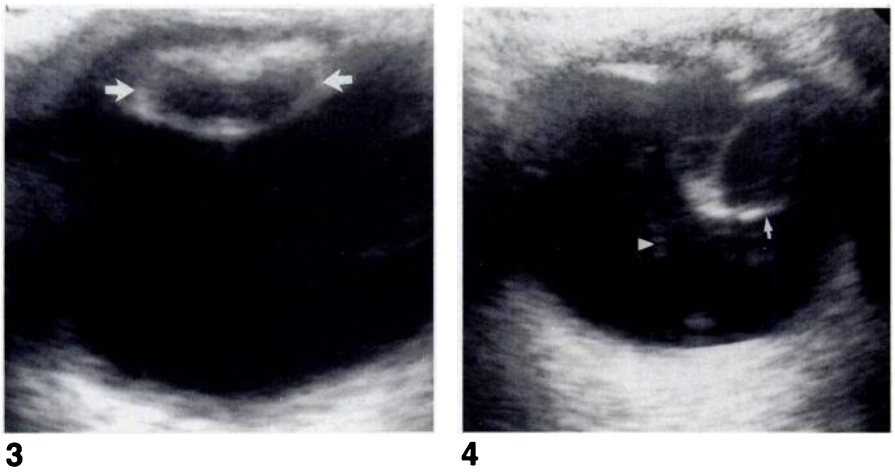

Fig. 3.—Cataract. Axial sonogram of patient with a moderately dense cataract (*arrows*) that precluded funduscopy. Sonogram shows normal vitreous and retina.

Fig. 4.—Lens dislocation. Axial sonogram shows lens (*arrow*) dislocated posteriorly as result of penetrating eye injury. Dynamic examination revealed that lens remained suspended by some zonular fibers in temporal aspect of eye. Some reactive vitreous hemorrhage and exudate (*arrowhead*) are apparent.

is incomplete, the vitreous remains bound at some point to the retina. This may occasionally resemble retinal detachment. However, on dynamic scanning, the detached vitreous should swirl away from the region of the optic disk (Fig. 6). If the vitreous remains attached near the optic disk, differentiation of the two conditions may be difficult. Echogenic vitreoretinal adhesions may be areas of epiretinal fibrosis and may be associated with traction retinal detachment [3] (Fig. 7).

Vitreous hemorrhage may occur spontaneously in vasoproliferative disease (e.g., sarcoidosis associated with uveitis) or as a result of trauma. Vitreous hemorrhage frequently obscures the retina from funduscopic visualization. Its appearance varies from a relatively homogeneous increase in echogenicity in fresh hemorrhage (Fig. 8) to echogenic stranding and scarring of the vitreous as time progresses (Fig. 9).

Retina/Retrohyaloid Space

In retrohyaloid hemorrhage, hemorrhage behind the vitreous displaces the vitreous gel and capsule forward (Fig. 10).

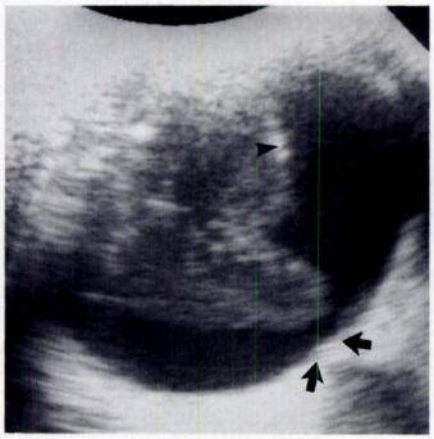

Fig. 5.—Vitreous detachment. Axial sonogram shows posterior surface of detached vitreous as an echogenic line (*arrowhead*). Echogenic vitreous shows a characteristic swirling movement on dynamic scanning. Vitreous is not attached at site of optic nerve head (*arrows*).

Fig. 6.—Retinal vs vitreous detachment. Axial sonogram shows retinal detachment (*arrowheads*) that was diagnosed during dynamic scanning because it remained bound at optic disk. Vitreous exudate (*arrow*) also is apparent, but this material swirled away from optic disk with eye movement.

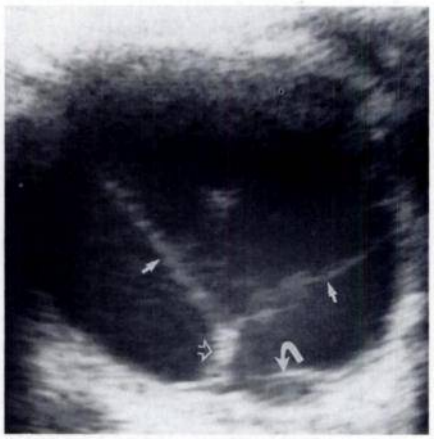

Fig. 7.—Chronic vitreous hemorrhage and detachment. Axial sonogram shows fibrous scar (*open arrow*) extending from detached vitreous (*solid straight arrows*) to posterior surface of globe. Scar has caused focal retinal detachment (*curved arrow*). Small subretinal hematoma also is visible.

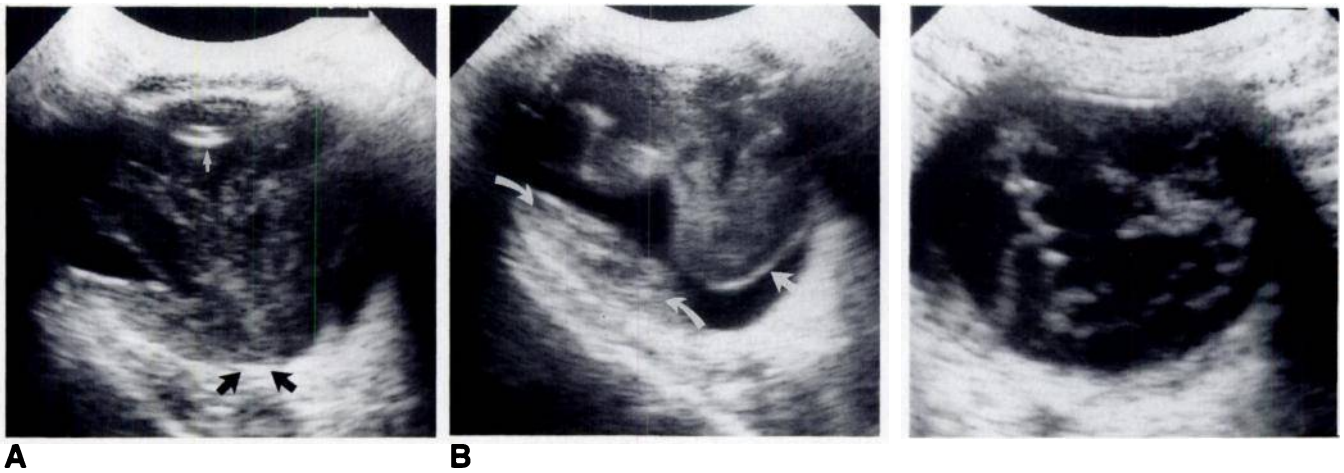

A **B**

Fig. 8.—Acute vitreous hemorrhage.

***A*, Axial sonogram shows echogenic material that swirled away from region of optic disk (*black arrows*) on dynamic scanning. Cataractous lens (*white arrow*) obscured funduscopic examination.**

***B*, Axial sonogram of another patient shows extensive vitreous exudate and detachment. Note line of detached vitreous (*straight arrow*). Collection of subretinal echogenic material is beneath retina (*curved arrows*), which was immobile. At surgery, this was found to be a large subretinal hemorrhage.**

Fig. 9.—Chronic vitreous hemorrhage. Axial sonogram shows dense vitreous stranding as a result of vitreous hemorrhage after trauma. These strands were almost totally immobile on dynamic scanning.

During dynamic scanning, the homogeneously echogenic blood swirls to and fro but is confined behind by the retina and in front by the vitreous capsule.

The retina is attached at two points: the ora serrata anteriorly and the optic disk posteriorly. At the ora serrata, the sensory retina is fused with the retinal pigment epithelial and choroid. This adhesion acts as a barrier to spread of retinal detachment anterior to the pars plana, the flat posterior part of the ciliary body.

Detachment may occur at any site, but even with complete detachment, the retina always remains bound at the ora serrata and optic disk [4]. Retinal detachment may be focal (Figs. 11 and 12) or complete (Fig. 13). It may be mobile or fixed during dynamic scanning. This information is relevant clinically for prognosis after surgery; mobile detachments have a better outcome. The angle formed between the leaves of detached retina may be open or closed, depending on the degree of vitreous retraction. Closed-angle detachments are more difficult to treat surgically. In chronic retinal detachment, cysts may form on the retina (Fig. 14).

Choroid

The choroid may also detach as a result of trauma or as a postoperative complication. In this condition, the choroid balloons into the eye (Fig. 15). The choroid protrudes into

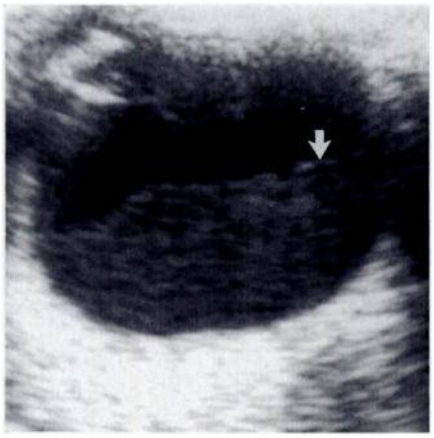

Fig. 10.—Retrohyaloid hemorrhage. Axial sonogram shows line of detached vitreous capsule (*arrow*) lying anterior to retrohyaloid hemorrhage. Echogenic blood showed movement during dynamic scanning but remained confined anteriorly by vitreous capsule and posteriorly by retina.

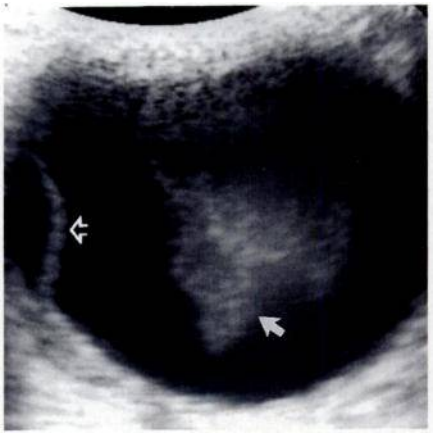

Fig. 11.—Focal retinal detachment (*open arrow*) and vitreous hemorrhage (*solid arrow*) shown by axial sonogram. This vitreous hemorrhage was mobile on dynamic scanning.

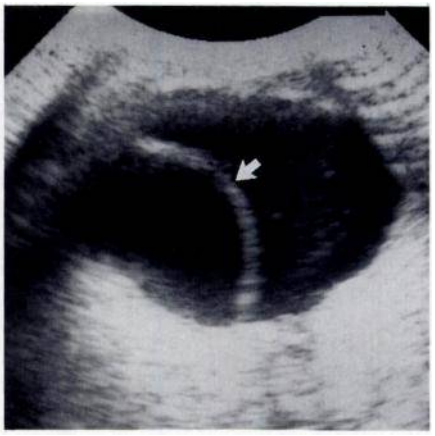

Fig. 12.—Focal bullous retinal detachment (*arrow*) shown by axial sonogram. Retina is ballooned into eyeball and considerable subretinal fluid is present. This type of retinal detachment can be difficult to differentiate from choroidal detachment solely on the basis of sonographic findings.

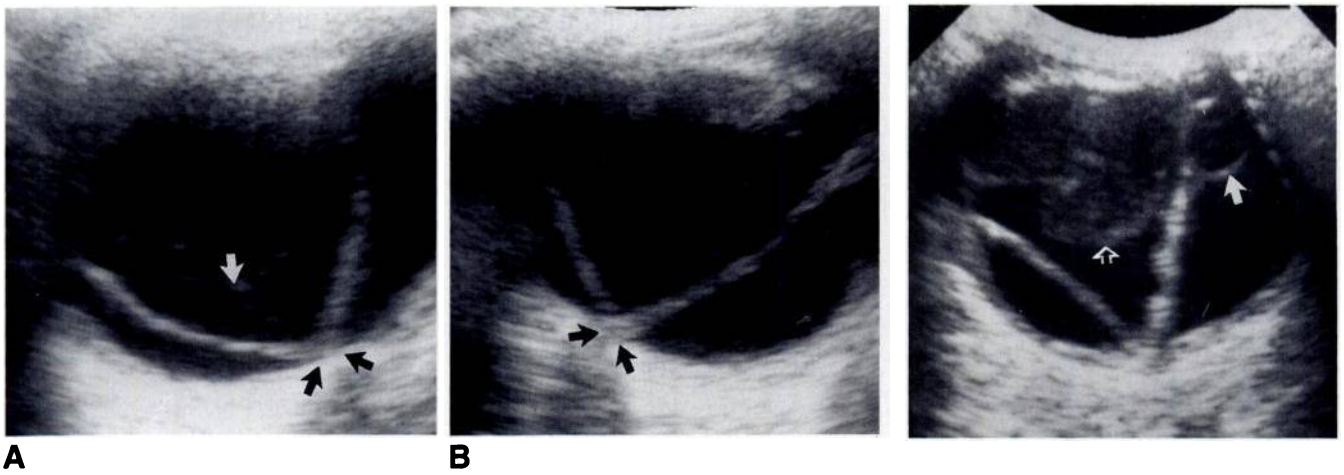

Fig. 13.—Complete retinal detachment.
***A* and *B*, Axial sonograms of eye looking to right (*A*) and eye looking to left (*B*) show some vitreous echoes (*white arrow*). Retina remains attached at optic disk during dynamic scanning (*black arrows*). A dense cataract (*not shown*) precluded funduscopy in this patient. During dynamic scanning, detached retina was relatively mobile, a good prognostic factor for successful surgery.**

Fig. 14.—Chronic fixed retinal detachment that was immobile on eye movement. Axial sonogram shows cyst (*solid arrow*), and vitreous exudate (*open arrow*) is also present.

the vitreous in a biconvex manner that can be seen in all planes of imaging. During dynamic scanning, this appearance does not change. The choroid is fixed just anterior to the ora serrata and posteriorly at some distance anterior to the optic disk.

Many tumors may metastasize to the choroid. Choroidal metastases may be sonographically indistinguishable from malignant melanoma if single. However, they are frequently multiple (Fig. 16), and then the diagnosis of metastases is relatively certain. They tend to be more hyperechoic than melanoma. During dynamic scanning, they move with the eye and do not change shape. No anterior adhesion between the choroid and the sclera is present, so choroidal detachments invariably progress anteriorly to involve the ciliary body [4].

Optic Disk and Nerve

Optic disk drusen is a benign condition in which hyaline material accumulates in the optic nerve head and calcifies. This results in an echogenic focus centered at the optic disk, which casts an acoustic shadow if heavily calcified (Fig. 17).

Optic nerve coloboma is congenital failure of fusion between the sclera and the choroid at the site of insertion of the optic nerve. This results in a defect at the optic disk site, which communicates with the vitreous chamber (Fig. 18).

Malignant Melanoma

Malignant melanomas are generally rounded or shaped like a collar stud, and they often have inhomogeneous internal echogenicity. They do not change shape during dynamic scanning. Many grow slowly, and the clinician may elect to follow up the patient with sonography, which allows accurate measurement of the transverse diameter and particularly of the anteroposterior dimension (height) of the melanoma (Fig. 19). Height is important, as this measurement cannot be made by funduscopic examination. The location of the lesion with respect to the optic disk is also clinically significant. These lesions often cause retinal detachment (Fig. 20) and may cause visual loss.

15

Fig. 15.—Choroidal detachment. Choroid detaches into globe in a biconvex manner that can be seen on both axial and longitudinal sonograms. On this axial scan, choroid remains bound anteriorly just anterior to ora serrata, but posteriorly its point of fixed attachment (*white arrows*) is at some distance anterior to optic disk. Note optic nerve (*black arrow*).

16

Fig. 16.—Choroidal metastases from lung carcinoma. Axial sonogram shows metastases as echogenic masses arising from wall of globe and protruding into vitreous. This 42-year-old man first had loss of vision and then had two choroidal metastases detected sonographically.

17

Fig. 17.—Optic disk drusen. Axial sonogram shows echogenic focus at optic nerve head (*white arrow*). Lesion has associated acoustic shadowing (*black arrows*) caused by calcium in drusen.

18

Fig. 18.—Optic nerve coloboma. Axial sonogram shows large defect in optic nerve that is grossly expanded. Note communication of expanded optic nerve with vitreous chamber (*straight arrows*). *Curved arrows* outline dimensions of expanded optic nerve containing echogenic material.

Fig. 19.—Small malignant melanoma. Axial sonogram shows small malignant melanoma on posterior of retina. Very small melanomas (2 mm in height) such as this one are best shown sonographically.

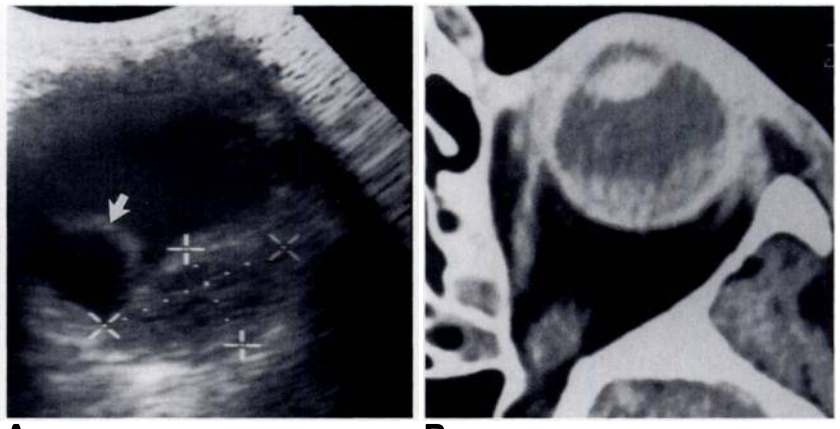

A B

Fig. 20.—Large malignant melanoma.

A, Axial sonogram shows large melanoma measuring 8 mm in height by 13 mm in transverse diameter and secondary retinal detachment (*arrow*).

B, Contrast-enhanced axial CT scan (2-mm slice thickness) shows difficulty in differentiating margin of melanoma from associated retinal detachment. MR imaging may have similar difficulties.

REFERENCES

1. Wilms G, Marshal G, Van Fraeyenhoven L, et al. Shortcomings and pitfalls of ocular MRI. *Neuroradiology* **1991**;33:320–325
2. Fisher YL, Slakter JS, Friedman RA, Yannuzzi LA. Kinetic ultrasound evaluation of the posterior vitreoretinal interface. *Ophthalmology* **1991**; 98:1135–1138
3. McLeod D, Restori M. Ultrasonic examination in severe diabetic eye disease. *Br J Ophthalmol* **1979**;63:533–538
4. Kanski JJ. *Clinical ophthalmology.* 2nd ed. London: Butterworth, **1989**:262

This article has been cited by:

1. Donna Napier. 2024. Ultrasound of the eye – Part 2: Fundamentals of posterior wall detachment. *Sonography* **11**:4, 329-339. [Crossref]
2. Amit Gupta, Shilpa Khanna Arora, Rachna Seth, Rakesh Kumar, Manisha Jana. 2022. Paediatric orbital ultrasound: Tips and tricks. *Australasian Journal of Ultrasound in Medicine* **25**:4, 200-206. [Crossref]
3. Aslan Efendizade, Suraj Patel, Zerwa Farooq, Vinodkumar Velayudhan. Imaging the Pediatric Patient 29-47. [Crossref]
4. Beatrice Hoffmann, Jesse M. Schafer, Christoph F. Dietrich. 2020. Emergency Ocular Ultrasound – Common Traumatic and Non-Traumatic Emergencies Diagnosed with Bedside Ultrasound. *Ultraschall in der Medizin - European Journal of Ultrasound* **41**:06, 618-645. [Crossref]
5. Maolin Pang, Sunao Liu, Fanchao Lin, Songlin Liu, Bei Tian, Wenli Yang, Xuejin Chen. Measurement of Optic Nerve Sheath on Ocular Ultrasound Image Based on Segmentation by CNN 1-5. [Crossref]
6. Rama Krishna Narra, Samardh Edara, Bhimeswara Rao P, Anusha Putcha. 2018. ROLE OF B-SCAN IN EVALUATION OF OCULAR AND EXTRA OCULAR PATHOLOGIES. *Journal of Evidence Based Medicine and Healthcare* **5**:48, 3307-3312. [Crossref]
7. Jeffrey Callard, James Kilmark, Hoodo Mohamed. 2017. Ocular Emergencies. *Physician Assistant Clinics* **2**:3, 519-536. [Crossref]
8. Marcela De La Hoz Polo, Anna Torramilans Lluís, Oscar Pozuelo Segura, Albert Anguera Bosque, Catalina Esmerado Appiani, Josep Maria Caminal Mitjana. 2016. Ocular ultrasonography focused on the posterior eye segment: what radiologists should know. *Insights into Imaging* **7**:3, 351-364. [Crossref]
9. Gavin Budhram, Jennifer Cronsell, Michele Schroeder, Jeremy Sautner, Elizabeth Schoenfeld, Tala Elia, Jennifer Friderici. 2015. Mobile vitreous opacities on ocular ultrasonography are not always pathologic: a cross-sectional survey in an asymptomatic population. *The American Journal of Emergency Medicine* **33**:12, 1808-1813. [Crossref]
10. S Loe, VA Dinh. 2014. Intra-Ocular Mass Diagnosed with Bedside Ultrasound. *Hong Kong Journal of Emergency Medicine* **21**:1, 48-50. [Crossref]
11. Keizo Tanitame, Takashi Sone, Yoshiaki Kiuchi, Kazuo Awai. 2012. Clinical applications of high-resolution ocular magnetic resonance imaging. *Japanese Journal of Radiology* **30**:9, 695-705. [Crossref]
12. Rosa M. Lorente-Ramos, Javier Azpeitia Armán, Araceli Muñoz-Hernández, José Manuel García Gómez, Susana Bilbao de la Torre. 2012. US of the Eye Made Easy: A Comprehensive How-to Review with Ophthalmoscopic Correlation. *RadioGraphics* **32**:5, E175-E200. [Crossref]
13. Pedro Seguí, Elena Elizagaray, Carlos Nicolau, Ximena Wortsman, Rosa Zabala, Jose Luís del Cura, Montserrat Domingo. Small Parts 109-157. [Crossref]
14. Daniel T. Ginat, Vikram S. Dogra. Future Considerations 201-207. [Crossref]
15. L.M. Sconfienza, F. Lacelli, A. Ardemagni, N. Perrone, M. Bertolotto, R. Padolecchia, G. Serafini. 2010. High-resolution, three-dimensional, and contrast-enhanced ultrasonographic findings in diseases of the eye. *Journal of Ultrasound* **13**:4, 143-149. [Crossref]
16. O. Bergès, P. Koskas, F. Lafitte, J.-D. Piekarski. 2006. Échographie de l'œil et de l'orbite avec un échographe polyvalent. *Journal de Radiologie* **87**:4, 345-353. [Crossref]
17. Tsung-Jen Wang, Chang-Hao Yang, Shu-Lang Liao, Tzyy-Chang Ho, Jen-Shang Huang, Chang-Ping Lin, Chung-May Yang, Muh-Shy Chen, Luke Long-Kuang Lin. 2003. Characteristic Ultrasonographic Findings of Choroidal Tumors. *Journal of Medical Ultrasound* **11**:2, 55-59. [Crossref]
18. Ellen Jorgensen. 1996. Sonographic Diagnosis of Reteinal Detachnents. *Journal of Diagnostic Medical Sonography* **12**:6, 287-294. [Crossref]